

## Article

# Preparation of Polypropylene Composites with Pyrolyzed Carbon Fibers Using an Internal Mixer

Dennis Müller <sup>1,\*</sup>, Matthias Bruchmüller <sup>1</sup> and Florian Puch <sup>1,2</sup>

<sup>1</sup> Plastics Technology Group, Faculty of Mechanical Engineering and Thuringian Center of Innovation in Mobility, Technische Universität Ilmenau, 98693 Ilmenau, Germany; matthias.bruchmueller@tu-ilmenau.de (M.B.); florian.puch@tu-ilmenau.de (F.P.)

<sup>2</sup> Thüringisches Institut für Textil- und Kunststoff-Forschung e.V., 07407 Rudolstadt, Germany

\* Correspondence: dennis.mueller@tu-ilmenau.de

**Abstract:** The use of pyrolyzed carbon fibers (pCFs) in the secondary raw material market is growing, but potential applications for pCFs are limited by their wool-like appearance. Common solutions are further processing into fiber mats or shredding and adding the fibers during compounding in twin-screw extruders (TSEs). In the latter process, the initial fiber length is usually reduced to less than 1 mm during compounding and further reduced during injection molding. Hence, this paper presents an alternative compounding approach by investigating if internal mixers (IMs) are suitable for retaining pCFs after compounding longer. First, the influence of the mixing sequence for adding pCFs to the mixing process of the resulting fiber length was investigated. Second, a design of experiments was carried out using a laboratory IM, considering the process parameters of rotational speed, mixing time, coupling agent content, initial fiber length, and chamber filling level. Third, the results obtained were scaled up and applied to a production-scale IM. Important findings are that the melting of the matrix polymer should occur before fibers are added. This results in fiber contents of 20 wt.%. To achieve higher fiber contents, small amounts of carbon fiber must be added during the melting process. The process parameters investigated had no significant influence on the resulting fiber length. Compounding with IM is suitable for an initial fiber length of up to 24 mm. A composite with carbon fibers from industrial offcuts (rCFs) prepared by TSE compounding was used to compare the mechanical properties of the injection-molded samples due to the non-availability of composites with pyrolyzed fibers. Compounding resulted in an improvement in the weight-average fiber length from 226  $\mu\text{m}$  (TSE) to 540  $\mu\text{m}$  (IM). However, this fiber length could not be preserved during injection molding, resulting in similar mechanical properties of both, the pCF composites prepared by an IM and the commercially available rCF composites.

**Keywords:** carbon fiber-reinforced thermoplastic; pyrolyzed carbon fiber; IM; fiber attrition; recycled carbon fiber; recycling; fiber length; mechanical properties



**Citation:** Müller, D.; Bruchmüller, M.; Puch, F. Preparation of Polypropylene Composites with Pyrolyzed Carbon Fibers Using an Internal Mixer.

*Recycling* **2024**, *9*, 115. <https://doi.org/10.3390/recycling9060115>

Academic Editors: Francesco Paolo La Mantia and Denis Rodrigue

Received: 2 September 2024

Revised: 29 October 2024

Accepted: 12 November 2024

Published: 22 November 2024



**Copyright:** © 2024 by the authors. Licensee MDPI, Basel, Switzerland. This article is an open access article distributed under the terms and conditions of the Creative Commons Attribution (CC BY) license (<https://creativecommons.org/licenses/by/4.0/>).

## 1. Introduction

Recently, fiber-reinforced composites with thermoplastic matrices have been gaining increasing attention. This is due to their potential advantages, such as excellent weight-specific mechanical properties, short cycle times, storability, repeated meltability, recyclability, good formability, and the use of alternative joining processes that enable automated large-volume manufacturing processes. These exceptional features make them applicable in numerous industries, including electronics, aerospace, automotive, transportation, military, energy, marine, sports and leisure, construction, medical, agriculture, recreation, industrial equipment, furniture, and more [1–5].

Carbon fiber composites on the market today predominantly consist of carbon fiber-reinforced thermosetting resins. During the curing process of thermosetting resins, intermolecular cross-linking occurs, resulting in the formation of a mesh structure. This

cross-linked structure significantly complicates the recycling process, as it becomes difficult to break down and repurpose the material [6]. The recovery of the fibers requires a material-friendly separation of the carbon fibers from the resin matrix. The high-temperature pyrolysis method offers high processing capacity and an enhanced recovery rate [7]. This approach allows for the recovery of long pyrolyzed carbon fibers (pCFs) that retain excellent mechanical properties as they preserve 94% of the tensile strength of the original fiber [8].

Maintaining the fiber length is of crucial importance when processing fiber-reinforced composites, as the resulting fiber length has a significant influence on the mechanical properties of the molded part [9,10].

The impact of fiber length shortening in the injection molding of glass fiber-reinforced PP was studied by Mohammad Karimi et al., who examined factors including screw speed, temperature, and fiber volume [11]. The findings show that higher screw speeds cause more damage to fibers, resulting in their shorter length, while increasing temperature preserves them due to decreased viscosity. The increase in fiber volume causes fiber interactions to intensify, leading to shorter lengths.

The fiber length, distribution, and orientation of long glass fibers were analyzed by Hou et al. during injection molding [12]. The shear rate was increased by high injection volume flow rates, resulting in fibers breaking more frequently, and 60–90% were less than 3 mm in length after plasticization.

Other publications concentrated less on the process parameters and more on enhancing the machine parameters. Inoue et al. examined a screw design that is fiber-friendly and discovered that the area between the feed and compression zones is where the most fiber degradation occurs, also confirmed by Huang et al. [13,14]. Similar approaches were taken by Ville et al. [15]. As the results of Huang et al. indicate, the use of specially designed machines is necessary to achieve the longest possible fiber length in injection molding.

Theoretical models for the description of fiber shortening are not the focus of this work but can be found in previous publications [16,17].

There are few theories and publications on fiber shortening in carbon fibers during TSE and injection molding. In the work of Malatyali et al. from 2021, a model for fiber shortening of CF in TSE is established [18]. Further publications then focused on the fiber shortening of recycled CF (fiberballs and chopped fibers) [19,20]. Shear rate, screw speed, fiber content, and fiber density were varied.

The study by Unterweger et al. examines how fiber length and fiber content affect the mechanical properties of injection-molded CF short fibers [21]. The composites' tensile strength, tensile modulus, and notched impact strength were strongly correlated with the weight-average fiber length. Composites with 15 vol% CF showed the best mechanical performance.

Höftberger et al. clearly show that, in addition to shortening fibers in the compounding step of TSE from 900 to 300  $\mu\text{m}$ , another shortening occurred during injection molding of approximately 500 to 250  $\mu\text{m}$  [22]. Shortening the residence time in the compound could lead to a slight increase in fiber length after compounding, which in turn affected the mechanical properties after injection molding by 5–10%.

Published work on fiber shortening in the internal mixer is limited.

Simizu et al. used a tangential internal mixer to simulate the kneading zone of a TSE with glass fibers [23,24]. Fiber damage was identified as a result of the number of rotations and shear stress. A similar approach was used by Inceoglu et al., comparing a tangential IM with two TSEs when using PA6 [25]. The fiber shortening was caused by screw or rotor speed and mixing time.

The processing of recycled, pyrolyzed CF on an intermeshing IM is a completely new approach.

The IM compounding process originated in the industrial rubber products and tire industry. It has been widely used and established for decades as the standard method for producing rubber compounds [26]. The process can also be used for compounding fibers in thermoplastics, although there is still a lack of published data [27].

The aim of this paper is to investigate the influence of compounding pCF composites using an IM. Hence, the influence of the processing parameters on the resulting fiber length is examined. Furthermore, the fiber length after compounding with an IM is compared to commercially available rCF composites prepared by the established compounding process using twin-screw extrusion.

## 2. Results

### 2.1. Mixing Sequence for Processing pCFs

Three different times of addition were investigated, as described in Section 4.3.3. Figure 1a displays an optical microscopy image of a calcined fiber sample after using the mixing sequence I shown in Figure 10.

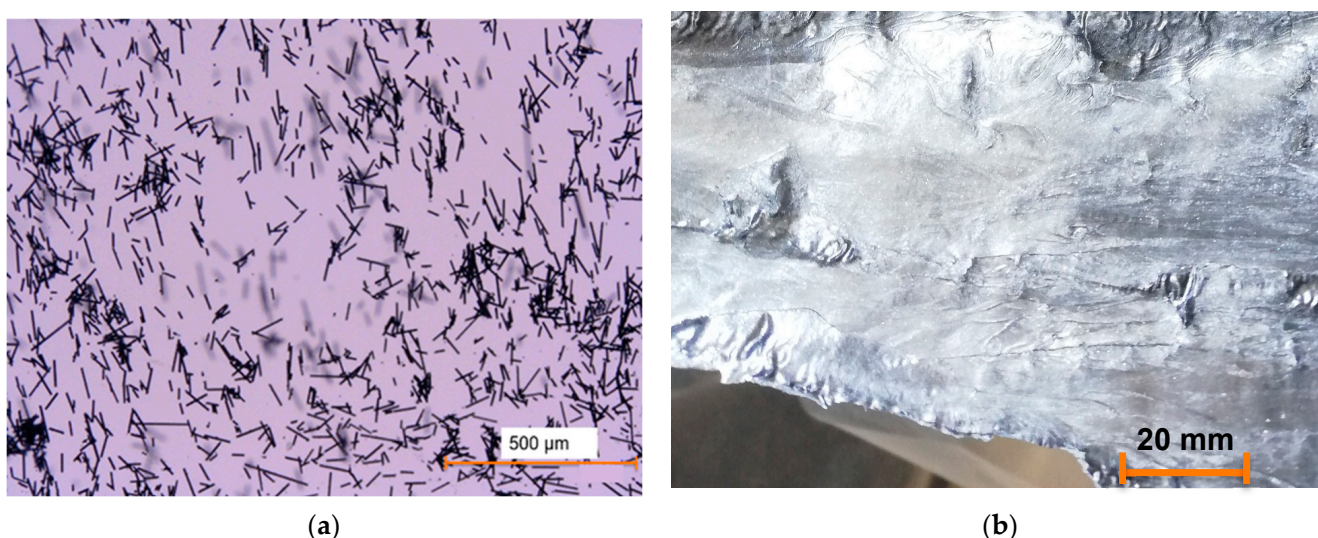


**Figure 1.** Comparison of calcined samples from the IM taken for different fiber addition times: (a) optical microscopy image of pCFs after mixing sequence I; (b) image of the PP-pCF composite after mixing sequence I.

Fiber length measurements, as described in Section 4.3.1, exhibited a significant decrease in fiber length from the initial fiber length of 6 mm. The number-average fiber length for the pCF composites was 51  $\mu\text{m}$ , while the weight-average fiber length was 79  $\mu\text{m}$ . A picture of the composite sample after internal mixing depicted in Figure 1b shows the mixing quality of this sequence as an example. The investigated sections did not contain fiber nests or unincorporated fibers, and the fiber content of the samples was 20%.

After compounding using mixing sequence II (Figure 2a), an increase in the number-average fiber length from 51  $\mu\text{m}$  to 139  $\mu\text{m}$  and in the weight-average fiber length from 79  $\mu\text{m}$  to 282  $\mu\text{m}$  was observed. This process can be operated independently of fiber preservation due to the absence of fibers during the melting. High rotation speeds and long mixing times are possible in the melting phase. On the other hand, the fiber–fiber interactions are minimized by the shorter mixing time. The disadvantage of the later addition is a low initial chamber filling volume, which decreases the shear forces during the melting of the polymer. Consequently, the time until PP was molten increased from 100 to 300 s. pCFs are visible on the surface of the composite sample in Figure 2b. Compared to mixing sequence I, an increase in the amount of unincorporated material was observed, resulting in a slightly lower fiber content of 19.3 wt.% in the composite.

The results of mixing sequence III are shown in Figure 3b, showing that fiber bundle sections are not well incorporated and distributed in the composite.

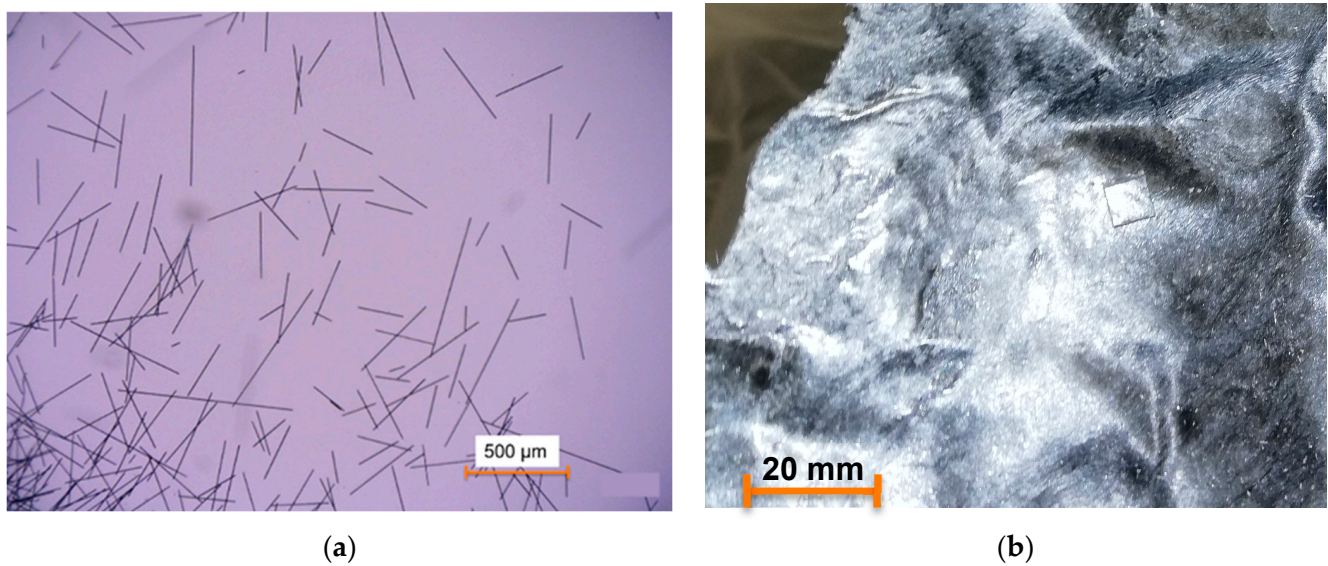


**Figure 2.** Comparison of calcined samples from the IM taken for different fiber addition times: (a) optical microscopy image of pCFs after mixing sequence II; (b) image of the PP-pCF composite after mixing sequence II.

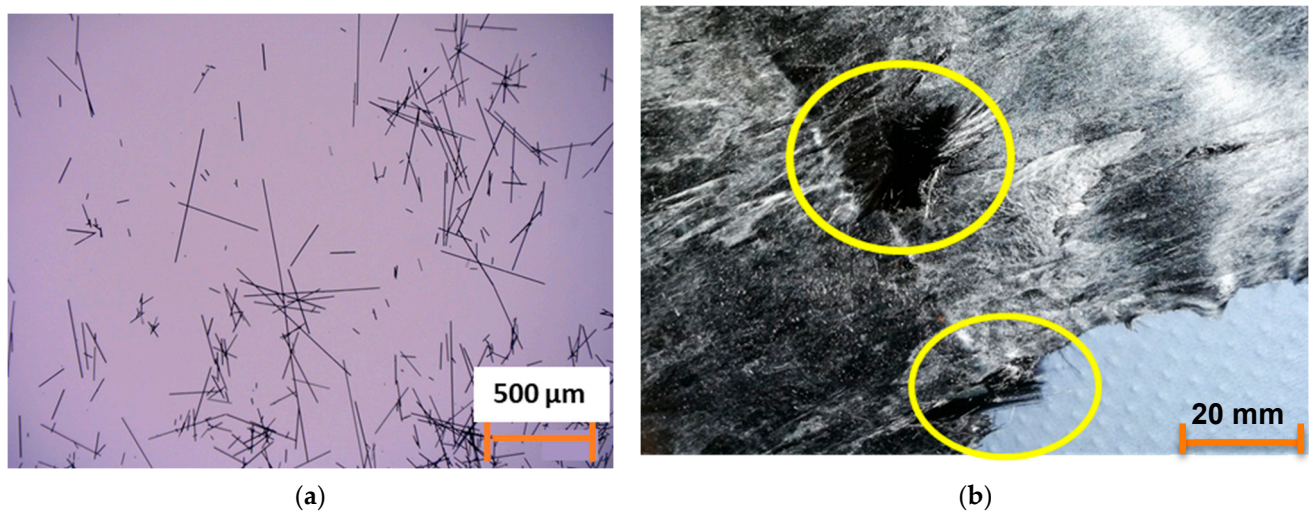


**Figure 3.** Comparison of calcined samples from the IM taken for different fiber addition times: (a) optical microscopy image of pCFs after mixing sequence III; (b) image of the PP-pCF composite after mixing sequence III: undistributed fiber bundles on the surface.

Hence, it may be concluded that the mixing quality of mixing sequence III was lower than the previous mixing sequences I and II. Additionally, the resulting number- and weight-average fiber lengths of 115  $\mu\text{m}$  and 222  $\mu\text{m}$ , respectively, were less than the fiber length obtained by mixing sequence II.

A comparison of the weight-average fiber length of commercially available composites produced with rCFs by TSE and the PP-pCF composites prepared by internal mixing using mixing sequence II is shown in Figure 4.

For both CF composites (TSE with rCFs and IM with pCFs after sequence II), the largest proportion of fibers had a measured fiber length in the range of 50–75  $\mu\text{m}$ , whereby most of the fibers were between 50 and 75  $\mu\text{m}$  long for the IM and between 75 and 100  $\mu\text{m}$  for the TSE. Both composites had a similar range of 125–300  $\mu\text{m}$ , and the IM composite had a greater proportion of long fibers at a fiber length of over 325  $\mu\text{m}$ . However, the proportion

of fibers over 350  $\mu\text{m}$  was only 4% higher than that of the commercial composites, which was further increased through process optimization, as discussed in the next sections.

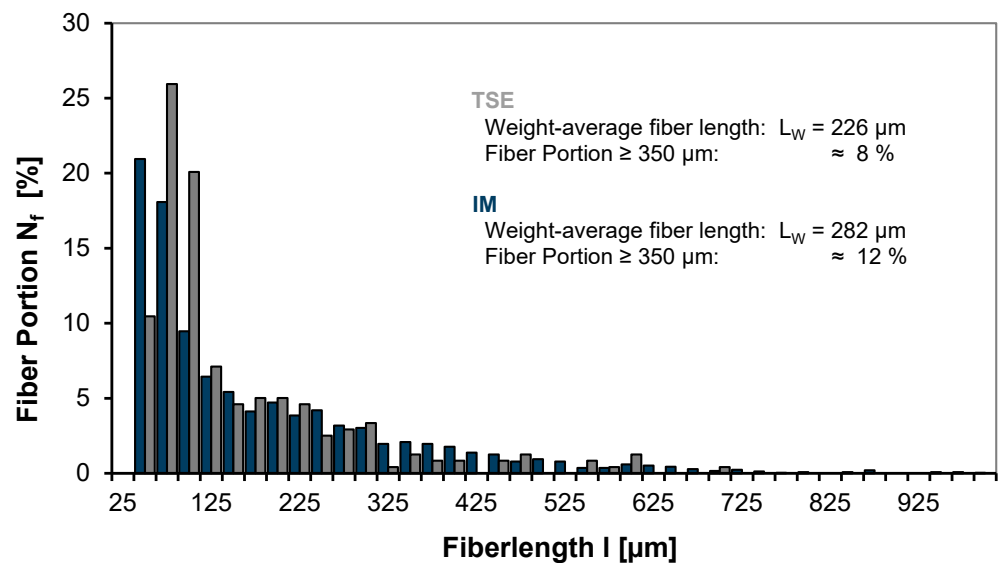


**Figure 4.** Histogram of the fiber length distributions of PP composites with 20 wt.% rCFs (prepared by TSE) and pCFs (prepared by IM).

2.2. Design of Experiments for Laboratory IM

2.2.1. One-Factor-at-a-Time Experiments for Laboratory IM

The influence of other process parameters on the resulting number- and weight-average fiber length are given in Table 1.

**Table 1.** One-factor-at-a-time results for laboratory IM.

Process Parameter	Value	Number-Average Fiber Length [ $\mu\text{m}$ ]	Weight-Average Fiber Length [ $\mu\text{m}$ ]
Mixing time	42 s	$125 \pm 13$	$340 \pm 75$
Mixing time	120 s	$142 \pm 16$	$251 \pm 49$
Chamber filling level	66%	$51 \pm 8$	$181 \pm 22$
Chamber filling level	78%	$127 \pm 21$	$264 \pm 71$
Initial fiber length	6 mm	$141 \pm 19$	$254 \pm 17$
Initial fiber length	24 mm	$86 \pm 4$	$272 \pm 12$

The results show that the mixing time had a noticeable influence on the fiber length in the PP-pCF composite. Additional measurements with 60 s, 80 s, and 100 s were similar to the fiber length at 120 s mixing time. Thus, a mixing time of 42 s was the shortest setting for low fiber damage without worsening the incorporation of pCFs into the matrix.

Longer fibers were observed at higher chamber filling levels, but at 78%, the process was not stable. Hence, the fiber content in the composite was reduced by 2–3 wt.%, and fiber nests from incompletely dispersed fiber bundles were observed on the surface, compared to Figure 13. Therefore, this process parameter was studied in greater detail, as discussed in Section 3.2, with a range of 68–73%, along with the initial fiber length of 12–24 mm. Table 1 shows a slight difference in fiber length in the investigated range of the initial fiber length. A full-factorial experimental plan was employed to determine the correlation between the initial fiber length, the chamber filling level, and the resulting fiber length to confirm a possible linear progression.

### 2.2.2. 2<sup>2</sup> Design of Experiments for Chamber Filling Level and Initial Fiber Length

The results of the full-factorial experimental plan are shown in Figure 5. The parameter’s standardized effect must exceed the calculated threshold of 2.306 to be considered statistically significant. This threshold was determined using a 95% confidence interval. Figure 5 demonstrates that neither the chamber filling level nor the initial fiber length significantly affected the resulting weight-average fiber length. Consequently, variations in these process parameters did not have a significant influence on the weight-average fiber length. The results for the number-average fiber length had comparable or worse values, so in what follows, only the weight-average results are discussed.

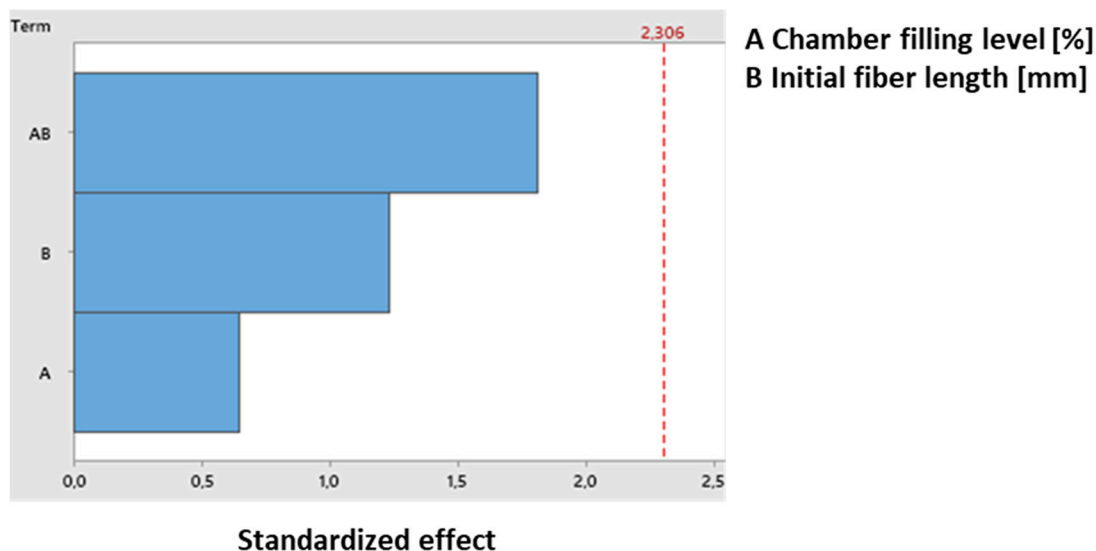


**Figure 5.** Standardized effects of the process parameters chamber filling level and initial fiber length on the resulting weight-average fiber length, 95% confidence interval.

The chamber filling level of 73% yielded no significant results in the area of fiber shortening but showed the best results in the area of mixing quality; thus, it was utilized for further experiments. The initial fiber length of 24 mm had no significant advantage over 6 or 12 mm. Since the longest possible initial fiber length was used to investigate IM processing, 24 mm long fibers were utilized.

### 2.3. Mechanical Properties

The resulting mechanical properties of the composites were determined in tensile and impact tests. The examination of ten injection-molded samples per composite included an analysis of tensile modulus, tensile strength, and Charpy impact strength. The laboratory-scale IM process parameters were projected onto a production-scale IM using the results from Section 2.2. The chamber filling level of 73% and the initial fiber length of 24 mm were adopted, and the mixing time was set to 140 s. The rotor speed had to be adopted and varied between 30 and 60 rpm to avoid significant cooling and freezing of the PP during the addition of pCFs. The results for the composites from laboratory- and production-scale IMs are shown in Table 2.

**Table 2.** Results of the tensile and impact tests.

Compounding Equipment	Tensile Modulus [N/mm <sup>2</sup> ]	Tensile Strength [N/mm <sup>2</sup> ]	Charpy Impact Strength [kJ/m <sup>2</sup> ]
Laboratory-scale IM	5738 ± 381	83 ± 2.9	26.2 ± 1.2
Production-scale IM	6537 ± 356	100 ± 2.6	24.0 ± 1.3

Injection-molded parts from the production-scale IM showed an 800 N/mm<sup>2</sup> higher tensile modulus and 17 N/mm<sup>2</sup> higher tensile stress. The difference of 2.2 kJ/m<sup>2</sup> in Charpy impact strength was within the standard deviation of both values, meaning that the difference in impact strength was negligible. The standard deviation for the tensile modulus was 5.4% for the production-scale IM and 6.4% for the laboratory-scale IM; these values are high, so it can be assumed that fiber distribution or orientation is not homogeneous in the molded samples. A comparison of the resulting fiber length for both IMs is shown in Table 3.

**Table 3.** The resulting number- and weight-average fiber length after compounding.

Compounding Equipment	Number Average [ $\mu\text{m}$ ]	Weight Average [ $\mu\text{m}$ ]
TSE	97 $\pm$ 11	226 $\pm$ 69
Laboratory-scale IM	152 $\pm$ 21	585 $\pm$ 296
Production-scale IM	123 $\pm$ 38	445 $\pm$ 21

The resulting fiber length was higher for compounding using the IMs. The significantly increased standard deviation of the weight-average fiber length in the laboratory-scale IM can be explained by its more compact design. This caused the fibers to be subjected to greater shear stresses than in machines on a production scale, so the variations in fiber length were higher. Another source of error can be the statistical evaluation of the fiber length measurements. With a wide fiber length range of 10–2400  $\mu\text{m}$ , long fibers of 1000  $\mu\text{m}$  or higher can ensure that the remaining image section shows a high number of small-to-medium fiber lengths. These high differences in the measured fibers increase the difficulty of identifying the fiber length at one value, and therefore the density distribution curves should instead be compared.

### 3. Discussion

#### 3.1. IM Mixing Sequence for pCF Production: Summary of Key Findings and Future Work

The results in Section 2.1 show that although fibers can be added to the IM at any point in the process, only the addition shortly after the melting of the polymer matrix is effective in preserving the fiber length. This result therefore limits the maximum possible pCF content that can be added to PP with an IM. This is because an IM uses the shearing of the plastic granulates in the rotor chamber to achieve melting. The absence of fibers at the beginning of the melting process reduces the actual filling level in the chamber; therefore, more time and energy are required to melt the polymer. With a chamber filling level of 73%, after the addition of pCFs, the production of 20 wt.% pCFs was possible. Higher fiber contents failed because the PP granules did not melt. One solution to this limitation would be to add 2–5 wt.% pCFs in the melting step, which would introduce additional shear and heat conduction into the material. The validation of this approach is underway, including the extent to which the added proportion of fine short fibers influences the long fibers in the composite with fiber–fiber interactions.

#### 3.2. The 2<sup>2</sup> Design of Experiments for Chamber Filling Level and Initial Fiber Length: Summary of Key Findings and Future Work

The investigated IM process parameters that theoretically have an influence on the resulting fiber length after mixing had only a minor (ram pressure) or no significant influence (chamber filling level or initial fiber length) within the investigated limits, as demonstrated by the findings in Section 2.2.

The greatest influence was observed for the mixing time, but a statistically relevant influence was not found in the investigated range of 42–120 s. A further reduction in the mixing time was not possible, because the full incorporation and distribution of pCFs into PP could not be ensured. A further investigation of the intermediate steps of the mixing

time range of 42–54 s mixing time could provide further information on the optimum mixing time.

The process parameters for a maximum fiber length after compounding on the laboratory-scale IM within this study were therefore a rotor speed of 100 rpm, a chamber filling level of 73%, and 50 bar ram pressure. The resulting composite consisted of 77 wt.% PP, 3 wt.% AP, and 20 wt.% pCFs with an initial length of 24 mm. The mixing time after the addition of fibers to the IM was 42 s.

### 3.3. Mechanical Properties

Despite the higher fiber length in the PP-pCF composite (Figure 6), Section 2.3 shows that the mechanical properties were lower than that of the PP-rCF composite. This may be because only a fraction of the long fibers can be preserved in the composite during the injection molding of the test specimen.

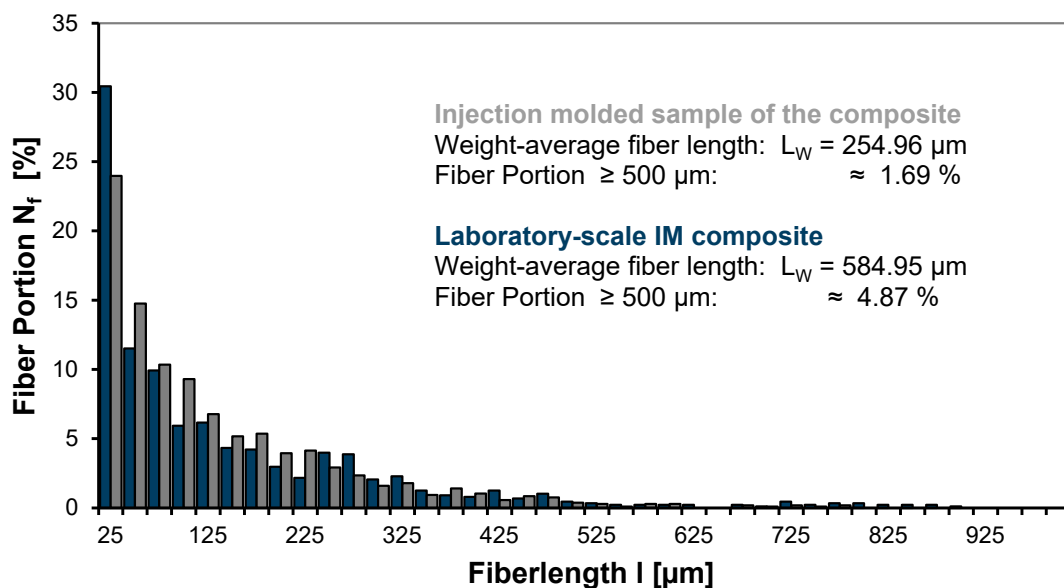


**Figure 6.** Histogram of the fiber length distribution of the laboratory IM composite before and after processing on an injection molding machine.

The shortening of the fibers to approximately 250 μm after injection molding was independent of the IM type (laboratory and production scale). Hence, the reduction in the fiber length of PP-pCF composites during injection molding should be investigated in future works to further exploit the potential of the PP-pCF composites.

## 4. Materials and Methods

### 4.1. Materials

Polypropylene (PP) with 20 mass percent recycled carbon fibers (rCFs) from Techno-Compound GmbH (Bad Sobernheim, Germany) was investigated as a TSE-compounded benchmark material (TechnoFiber PP CF20). The mechanical properties of the PP-rCF composite showed a tensile modulus of 3.4 GPa, a tensile strength at break of 99 MPa, and an elongation at break of 3%. Researchers' own measurements revealed a Charpy impact and notched impact strength of 28.6 kJ/m<sup>2</sup> and 1.5 kJ/m<sup>2</sup>, respectively.

The IM composite was prepared using a PP type HJ325MO (Borealis AG, Vienna, Austria) and pyrolyzed carbon fibers (pCFs) (CFK Valley Stade Recycling GmbH & Co. KG, Stade, Germany) from high-modulus (HM) applications. The unenforced matrix material showed a maximum tensile modulus of 1.6 GPa, tensile strength at break of 35 MPa, and an elongation at break of 9%. The Charpy notched impact strength was 2.0 kJ/m<sup>2</sup>. The used pCFs had an initial fiber length of 6, 12, and 24 mm. As an adhesion promoter (AP), HV Scona TSPP 10,213 GB (BYK-Chemie GmbH, Wesel, Germany) was used to improve

the surface of the fibers, which, after the pyrolysis process, has no adhesion promoter for bonding to the matrix polymer.

#### 4.2. Equipment

First, a laboratory-scale IM with a 5 L chamber volume type GK5E (Harburg-Freudenberger Maschinenbau GmbH, Hamburg, Germany) with PES5 intermeshing rotor blades was used. For the production of granules, a laboratory sheet and a mixing mill 300 × 700 (Harburg-Freudenberger Maschinenbau GmbH, Hamburg, Germany) were used to draw a fleece, and then shredding was performed with a GR 150 UC Band Granulator (Sagitta s.p.a., Vigevano, Italy).

Then, for investigations of the production scale, a 320 L IM type GK320E (Harburg-Freudenberger Maschinenbau GmbH, Hamburg, Germany) was utilized. Initially, this machine was modified for compounding natural fibers with thermoplastics so that water in the fibers could leave the chamber as steam (Harburg-Freudenberger Maschinenbau GmbH, Hamburg, Germany). After using the IM, a single-screw extruder type EAE 300/16D (Harburg-Freudenberger Maschinenbau GmbH, Hamburg, Germany) was utilized for the underwater granulation of the resulting composite.

Finally, an injection-molding machine type KM80 0080/00380/CX//04 MC6 (Krauss-Maffei GmbH, Munich, Germany) with an 80 t closing force was used to produce the test specimens. The following settings were used to produce the test specimens: cylinder temperature 230 °C, decreasing; injection speed, 20 cm<sup>3</sup>/s; screw speed, 150 rpm; back pressure, 20 bar; holding pressure, 450 bar for 4 s; and injection pressure, approximately 950 bar.

The fiber distribution was investigated with a digital microscope type VHX-5000 (KEYANCE DEUTSCHLAND GmbH, Neu-Isenburg, Germany) and an optical microscope type Stemi 2000-C (Carl Zeiss AG, Oberkochen, Germany).

#### 4.3. Methods

##### 4.3.1. Fiber Length Measurement and Sample Preparation

In the literature, the number- and weight-average fiber length are usually used as parameters for the quantitative evaluation of the fiber length distribution. The number-average fiber length  $L_N$  corresponds to the arithmetic mean of the distribution and can be determined via the total number of all evaluated fibers  $n$  and the length  $L_i$  and frequency  $n_i$  of the individual fibers [28]:

$$L_N = \frac{\sum_{i=0}^n n_i \cdot L_i}{n}, \quad (1)$$

$L_N$  = number-average fiber length;

$n_i$  = number of fibers;

$L_i$  = fiber length;

$n$  = total number of all evaluated fibers.

The weight-average fiber length  $L_W$  also results from the total number of measured fibers  $n$  as well as the fiber length  $L_i$  and the fiber frequency  $n_i$  of the individual fibers, but the square of the individual fiber length  $L_i$  leads to the distortion of the measurement results. Since the fibers are assigned a higher weighting proportional to their length  $L_i$ , long fibers have a greater significance in the weight-average fiber length  $L_W$ , analogous to the influence of the fiber length on the mechanical properties [28].

$$L_W = \frac{\sum_{i=0}^n n_i \cdot L_i^2}{\sum_{i=0}^n n_i \cdot L_i}, \quad (2)$$

$L_W$  = weight-average fiber length.

Fibers were obtained from the composites or injection-molded samples by calcination according to DIN EN ISO 1172 [29]. Three subsamples were taken from each sample and dispersed on a slide by adding decanol. The fiber length was measured on three

different images per subsample as shown in Figure 7. At least 500 fibers were analyzed per subsample.

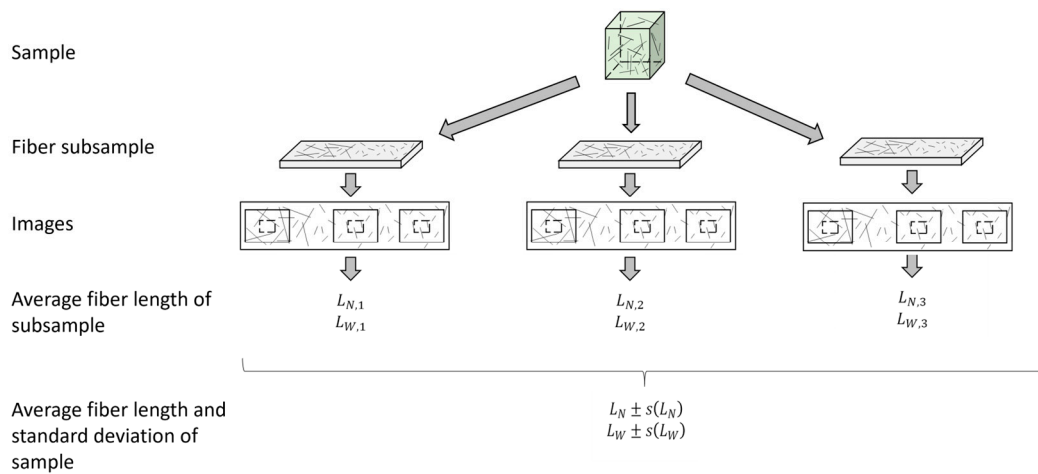


**Figure 7.** Determination of the number- and weight-average fiber length. [Figure adopted from [28]].

#### 4.3.2. Description of the Used IM

The IM is mainly used in rubber processing but thermoplastics and thermoplastic elastomers can also be processed. During the mixing process, a composite is created from two or more starting materials. Figure 8 shows an IM with intermeshing rotor systems, while Figure 9 shows the used blades in more detail.

The raw materials for the plastic composite are fed into the feed hopper and are then transferred to the mixing chamber using a ram. The pneumatically or hydraulically operated ram is not permanently mounted but is pressed onto the composite with constant pressure. This prevents large load peaks during the mixing process.

The mixing chamber consists of two end frames, two mixing chamber halves, and a rotor system. The rotor system consists of two cylindrical rotor bodies with two to six blades each; the number of blades in this investigation was two. The rotors mix the raw materials in the mixing chamber. As the rotors rotate in opposite directions, new materials that are fed in via the ram are introduced directly into the process. Once the mixing process is completed, the composite is conveyed to the discharge and ejected from the machine.

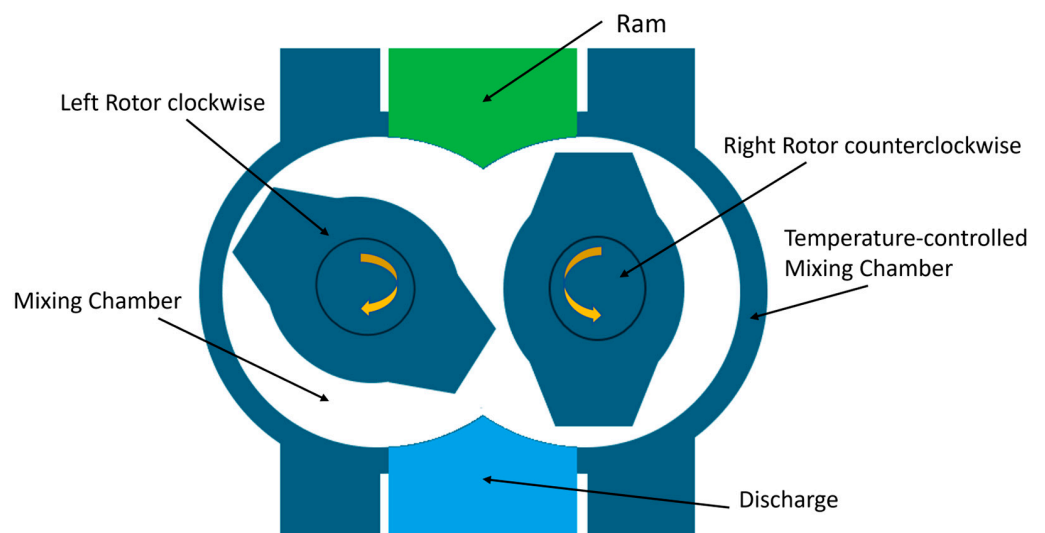


**Figure 8.** Sketch of the used IM with intermeshing rotor systems.

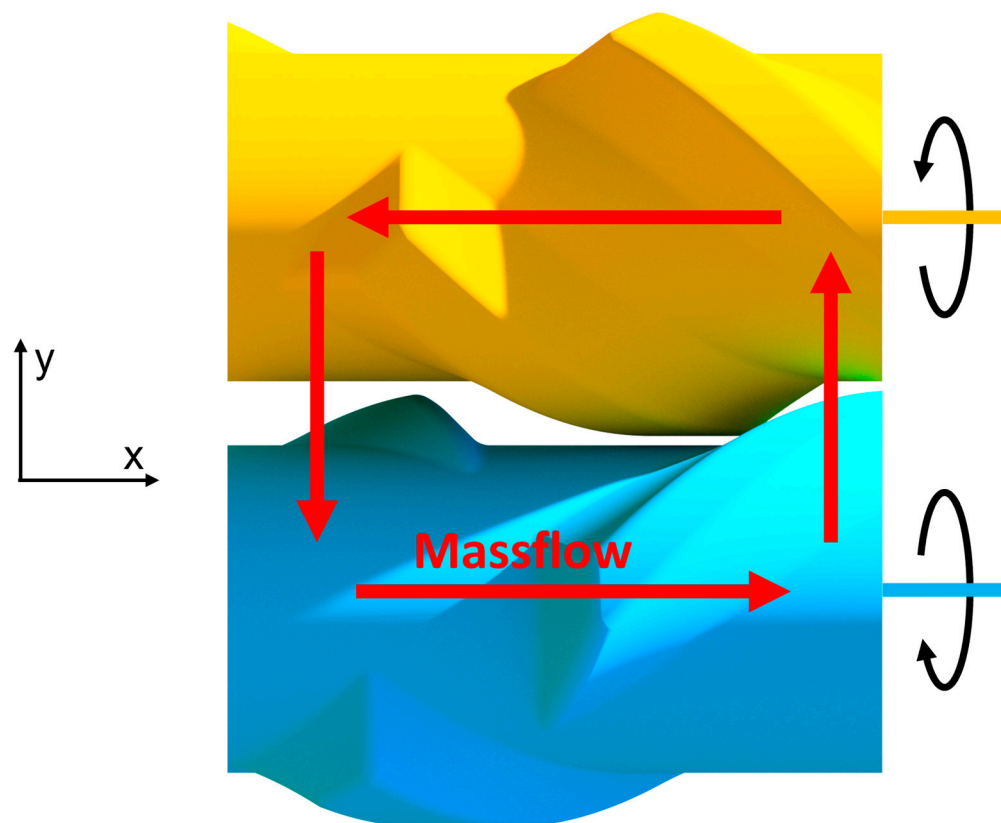


**Figure 9.** Sketch of mass flow with intermeshing rotor blades as used in laboratory- and production-scale IMs.

#### 4.3.3. Mixing Sequences for the IM

To produce a PP composite with pCFs, three possible mixing sequences were examined using the GK5E laboratory IM. All experiments were carried out at a rotor speed of 100 rpm. The IM chamber filling level was 68%. The composite consisted of 78 wt.% PP, 2 wt.% adhesion promoter (AP), and 20 wt.% pCFs with an initial length of 6 mm.

The mixing sequence during compounding using an IM has several degrees of freedom, for example, the time of addition of fibers and additives, ram position, and force. Before the process parameters for compounding the PP-pCF composite can be investigated systematically, the mixing sequence must be adopted for processing the PP-pCF composite to retain the fiber length.

In this study, three different mixing sequences were examined regarding mixing quality and fiber degradation. The mixing quality was estimated by visual inspection and the determination of the fiber content of the partial samples. Figure 10 shows mixing sequence I schematically, according to which fibers and granules were added together at the beginning of the mixing process, thus maximizing the shear on the fibers. The fiber length measurement was carried out as explained in Section 4.3.1.

Figure 11 schematically explains mixing sequence II, according to which the fibers were added after melting the PP granules so that the fibers would be exposed to less shear. The mixing time of the fibers in the plastic melt was set at 40 s and adjusted via the sensor data of the IM if needed.

In mixing sequence II, it was observed that the addition of the fibers after melting the PP resulted in unincorporated fiber nests at the bottom of the stamp. This reduced the total fiber content in the composite. Hence, the mixing sequence used was mixing sequence III shown in Figure 12. First, half of the fibers were added to the melt. After initial mixing, the stamp was raised so that unincorporated fiber nests would be released into the

melt together with the second half of the fibers. After further mixing, the composite was discharged and analyzed.

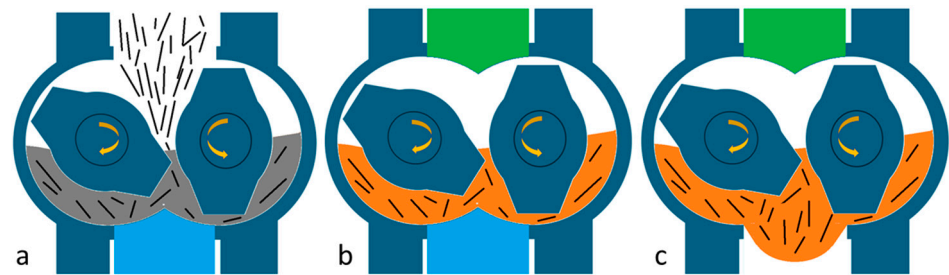


**Figure 10.** Mixing sequence I: (a) the addition of the fibers during the melting process of the polymer granules (gray = solid) in the IM; (b) the mixing of fibers and molten polymer (orange = liquid); (c) discharge of composite.

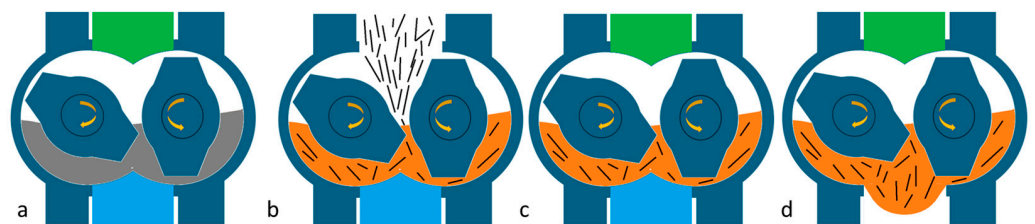


**Figure 11.** Mixing sequence II: (a) the melting process of the polymer granules (gray = solid) in the IM without fibers; (b) the addition of fibers to the molten polymer (orange = liquid); (c) the mixing of fibers and polymer; (d) discharge of composite.

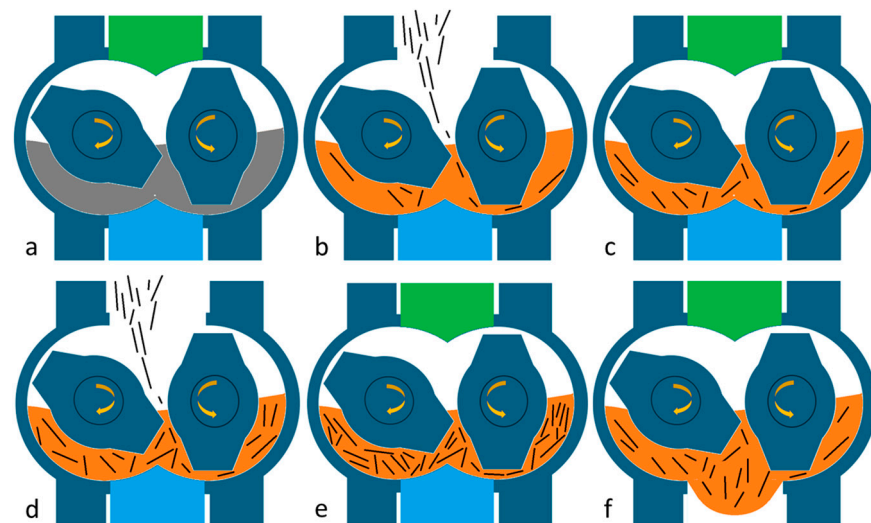


**Figure 12.** Mixing sequence III: (a) the melting process of the polymer granules (gray = solid) in the IM without fibers; (b) the addition of 10 wt.% fibers to the molten polymer (orange = liquid); (c) the mixing of fibers and polymer; (d) the addition of the remaining 10 wt.% fibers to the polymer; (e) the second mixing of fibers and polymer; (f) discharge of composite.

#### 4.3.4. Parameter Variations and Design of Experiments

A design of experiments approach was employed to assess the influence of process parameters on the properties of the composite and the fiber length. Several process parameters can influence the fiber length during compounding using an IM, for example, ram pressure, mixing time, chamber filling level, and initial fiber length. Hence, one-factor-at-a-time investigations were carried out to measure possible significances for the parameters first, as shown in Table 4.

**Table 4.** One-factor-at-a-time experiments for the laboratory IM.

Process Parameter	Value Range	Unit
Ram pressure	0, 25, 50	Bar
Mixing time	42, 60, 80, 100, 120	s
Chamber filling level	66, 68, 73, 75	%
Initial fiber length	6, 12, 24	mm

The fiber length in the composite did not change significantly when the ram pressure was changed from 0 to 50 bar. However, not all fibers were incorporated when the IM was operated without ram pressure, resulting in a reduction of 3–4 wt.% in the fiber content of the composite. To ensure the homogeneous mixing of PP and pCF, subsequent experiments were conducted at 50 bar ram pressure.

The different mixing times in the IM were determined by mixing curves recorded on the device. In Figure 13, a typical mixing curve for mixing sequence II is depicted. The mixing time only began after the ram was lowered. A decrease in the required current and power may indicate that all fibers were incorporated into the matrix material.

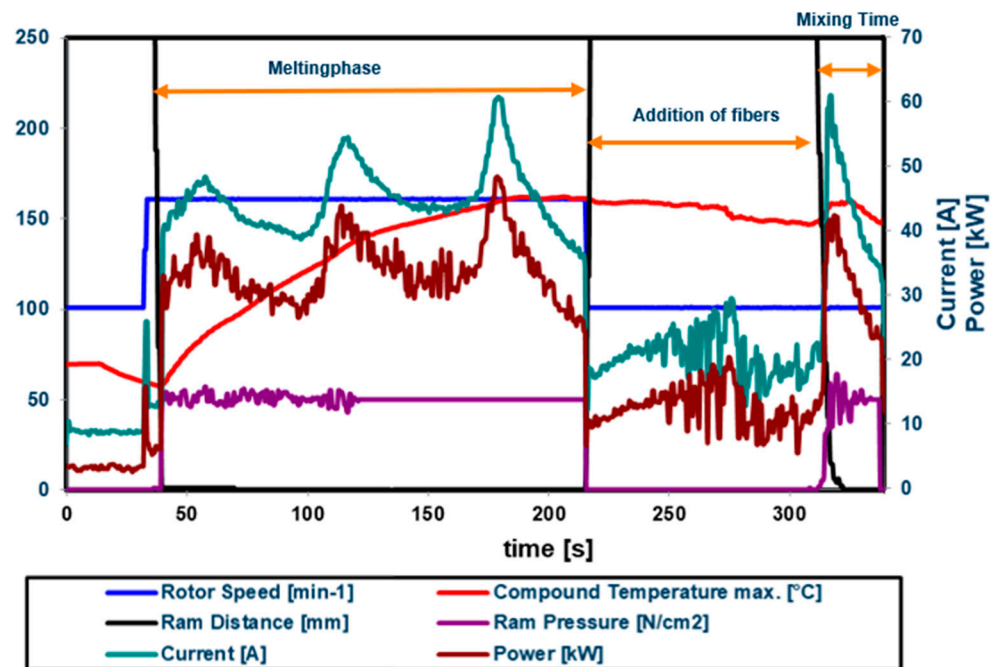


**Figure 13.** Mixing curve for mixing sequence II.

Subsequently, the most suspected parameters for fiber length degradation in the IM (chamber filling level and initial fiber length) were further investigated in a full factorial 2<sup>2</sup> experimental design (Table 5). Three repetitions of this experiment were conducted to achieve results that would be statistically reliable.

**Table 5.** The 2<sup>2</sup> design of experiments for chamber filling level and initial fiber length.

Process Parameter	Value -1	Value +1
Chamber filling level [%]	68	73
Initial fiber length [mm]	12	24

In addition to the weight-average fiber length of the samples, the target parameters for the evaluation of the DoE were the mechanical properties (tensile modulus, tensile strength, and impact strength) of the injection-molded parts.

#### 4.3.5. Mechanical Properties

In accordance with DIN EN ISO 527-4 (geometry type 1b) [30], injection-molded test specimens were used to determine the mechanical properties of all composites produced by internal mixing. All mechanical tests were performed using a universal testing machine (Shimadzu SFL-50KNAG, Shimadzu Corp., Kyoto, Japan). The experiments were carried out at room temperature with a testing speed of 1 mm/s until an elongation of 0.5% was reached; then, the testing speed was increased to 10 mm/s.

For the impact tests, the Charpy arrangement was chosen, and the test was carried out in the three-point support. The test specimens were standardized according to DIN EN ISO 179 [31] and were produced by injection molding. Test specimens were stressed in bending using a pendulum impact device. The impact mechanism according to DIN EN ISO 13802 [32] with an impact energy of 7.5 J involved deflection by 160° in these tests.

### 5. Conclusions

This study investigated the compounding of PP-pCF composites with laboratory- and production-scale IMs. It was shown that pCF addition should take place shortly after melting the PP to ensure a high mixing quality and low fiber deterioration. Further experiments showed that the reduction in fiber length was influenced by the mixing time, which additionally affected the quality of the mixture. A mixing time of 42 s on the laboratory-scale IM and 140 s on the production-scale IM was necessary to incorporate the pCFs into the matrix. A further reduction in this time could improve the fiber length but at the same time decrease the fiber content in the composite. The maximum initial fiber length was 24 mm. The mechanical properties of the composites prepared by internal mixing were on a similar level to the composites prepared by TSE despite higher fiber length after compounding. This is due to a fiber length reduction of 50% during the injection molding of the tensile test specimen. Further measurements should be conducted to examine the influence of injection molding on the fiber length of PP-pCF composites during processing to make use of the full potential of the longer fibers from the PP-pCF composites prepared by internal mixing.

**Author Contributions:** Conceptualization, D.M. and M.B.; methodology, D.M. and M.B.; validation, D.M.; formal analysis, F.P.; investigation, D.M.; resources, M.B.; data curation, D.M.; writing—original draft preparation, D.M.; writing—review and editing, M.B. and F.P.; visualization, D.M.; supervision, M.B. and F.P.; project administration, M.B. and F.P.; funding acquisition, M.B. All authors have read and agreed to the published version of the manuscript.

**Funding:** This study was supported by the Federal Ministry for Education and Research on the basis of a decision by the German Bundestag, grant number 033RK064B. We acknowledge the support for the publication costs from the Open Access Publication Fund of the Technische Universität Ilmenau. We thank the Thuringian Center of Innovation in Mobility for the infrastructural support.

**Institutional Review Board Statement:** Not applicable.

**Informed Consent Statement:** Not applicable.

**Data Availability Statement:** Data are contained within the article.

**Conflicts of Interest:** The authors declare no conflicts of interest.

### References

1. Kesarwani, S. Polymer Composites in Aviation Sector. *Int. J. Eng. Res. Technol.* **2017**, *6*, 518–525. [[CrossRef](#)]
2. Vaidya, U.K.; Chawla, K.K. Processing of fibre reinforced thermoplastic composites. *Int. Mater. Rev.* **2008**, *53*, 185–218. [[CrossRef](#)]
3. Shida, R.; Tsumuraya, K.; Nakatsuka, S.; Takahashi, J. (Eds.) Effect of automobile lightening by CFRP on the world energy saving. In Proceedings of the Ninth Japan International SAMPE Symposium, Tokyo, Japan, 29 November–2 December 2005.
4. Fukui, R.; Odai, T.; Zushi, H.; Ohsawa, I.; Uzawa, K.; Takahashi, J. (Eds.) Recycle of carbon fiber reinforced plastics for automotive application. In Proceedings of the 9th Japan International SAMPE Symposium, Tokyo, Japan, 29 November–2 December 2005.
5. Wan, Y.; Takahashi, J. Development of Carbon Fiber-Reinforced Thermoplastics for Mass-Produced Automotive Applications in Japan. *J. Compos. Sci.* **2021**, *5*, 86. [[CrossRef](#)]

6. Liu, J.; Wang, S.; Peng, Y.; Zhu, J.; Zhao, W.; Liu, X. Advances in sustainable thermosetting resins: From renewable feedstock to high performance and recyclability. *Prog. Polym. Sci.* **2021**, *113*, 101353. [[CrossRef](#)]
7. Guo, L.; Xu, L.; Ren, Y.; Shen, Z.; Fu, R.; Xiao, H.; Liu, J. Research on a two-step pyrolysis-oxidation process of carbon fiber-reinforced epoxy resin-based composites and analysis of product properties. *J. Environ. Chem. Eng.* **2022**, *10*, 107510. [[CrossRef](#)]
8. Ma, C.; Sánchez-Rodríguez, D.; Kamo, T. Influence of thermal treatment on the properties of carbon fiber reinforced plastics under various conditions. *Polym. Degrad. Stab.* **2020**, *178*, 109199. [[CrossRef](#)]
9. Fu, S.-Y.; Lauke, B.; Mäder, E.; Yue, C.-Y.; Hu, X. Tensile properties of short-glass-fiber- and short-carbon-fiber-reinforced polypropylene composites. *Compos. Part A Appl. Sci. Manuf.* **2000**, *31*, 1117–1125. [[CrossRef](#)]
10. Kim, Y.; Park, O.O. Effect of Fiber Length on Mechanical Properties of Injection Molded Long-Fiber-Reinforced Thermoplastics. *Macromol. Res.* **2020**, *28*, 433–444. [[CrossRef](#)]
11. MohammadKarimi, S.; Neitzel, B.; Lang, M.; Puch, F. Investigation of the Fiber Length and the Mechanical Properties of Waste Recycled from Continuous Glass Fiber-Reinforced Polypropylene. *Recycling* **2023**, *8*, 82. [[CrossRef](#)]
12. Hou, X.-Q.; Chen, X.-Y.; Liu, B.-C.; Chen, S.-C.; Li, H.-M.; Cao, W. Fracture and Orientation of Long-Glass-Fiber-Reinforced Polypropylene During Injection Molding. *Polym. Eng. Sci.* **2020**, *60*, 13–21. [[CrossRef](#)]
13. Huang, P.-W.; Peng, H.-S.; Hwang, S.-J.; Huang, C.-T. The Low Breaking Fiber Mechanism and Its Effect on the Behavior of the Melt Flow of Injection Molded Ultra-Long Glass Fiber Reinforced Polypropylene Composites. *Polymers* **2021**, *13*, 2492. [[CrossRef](#)] [[PubMed](#)]
14. Inoue, A.; Morita, K.; Tanaka, T.; Arao, Y.; Sawada, Y. Effect of screw design on fiber breakage and dispersion in injection-molded long glass-fiber-reinforced polypropylene. *J. Compos. Mater.* **2015**, *49*, 75–84. [[CrossRef](#)]
15. Ville, J.; Inceoglu, F.; Ghamri, N.; Pradel, J.L.; Durin, A.; Valette, R.; Vergnes, B. Influence of Extrusion Conditions on Fiber Breakage along the Screw Profile during Twin Screw Compounding of Glass Fiber-reinforced PA. *Int. Polym. Process.* **2013**, *28*, 49–57. [[CrossRef](#)]
16. Chen, H.; Cieslinski, M.; Baird, D.G. (Eds.) Progress in modeling long glass and carbon fiber breakage during injection molding. In *AIP Conference Proceedings*; AIP Publishing LLC: New York, NY, USA, 2015.
17. Kang, J.; Huang, M.; Zhang, M.; Zhang, N.; Song, G.; Liu, Y.; Shi, X.; Liu, C. An effective model for fiber breakage prediction of injection-molded long fiber reinforced thermoplastics. *J. Reinf. Plast. Compos.* **2020**, *39*, 473–484. [[CrossRef](#)]
18. Malatyali, H.; Schöppner, V.; Rabeneck, N.; Hanselle, F.; Austermeier, L.; Karch, D. A model for the carbon fiber breakage along the twin-screw extruder. *SPE Polym.* **2021**, *2*, 145–152. [[CrossRef](#)]
19. Malatyali, H.; Schöppner, V. Evaluation of a carbon fiber breakage model with reused chopped fiber. In Proceedings of the 37th International Conference of the Polymer Processing Society (PPS-37), Fukuoka City, Japan, 11–15 April 2022.
20. Malatyali, H.; Schöppner, V.; Hoemann, T. Investigation of the influence of process and screw configurations on fiber length for recycled carbon fiber. In Proceedings of the International Conference on Humans and Technology: A Holistic and Symbiotic Approach to Sustainable Development: Icht 2022, Kochi, Kerala, India, 17–22 January 2022.
21. Unterweger, C.; Mayrhofer, T.; Piana, F.; Duchoslav, J.; Stifter, D.; Poitzsch, C.; Fürst, C. Impact of fiber length and fiber content on the mechanical properties and electrical conductivity of short carbon fiber reinforced polypropylene composites. *Compos. Sci. Technol.* **2020**, *188*, 107998. [[CrossRef](#)]
22. Höftberger, T.; Dietrich, F.; Zitzenbacher, G.; Burgstaller, C. Influence of Fiber Content and Dosing Position on the the Mechanical Properties of Short-Carbon-Fiber Polypropylene Compounds. *Polymers* **2022**, *14*, 4877. [[CrossRef](#)]
23. Shimizu, Y.; Arai, S.; Itoyama, T.; Kawamoto, H. Experimental analysis of the kneading disk region in a co-rotating twin screw extruder: Part 2. glass-fiber degradation during compounding. *Adv. Polym. Technol.* **1997**, *16*, 25–32. [[CrossRef](#)]
24. Shimizu, Y.; Arai, S.; Itoyama, T.; Kawamoto, H. Experimental analysis of the kneading disk region in a co-rotating twin screw extruder: Part 1. Flow characteristics of the kneading disk region. *Adv. Polym. Technol.* **1996**, *15*, 307–314. [[CrossRef](#)]
25. Inceoglu, F.; Ville, J.; Ghamri, N.; Durin, A.; Valette, R.; Vergnes, B. (Eds.) A Study of Fiber Breakage During Compounding of Glass Fiber Reinforced Composites. In Proceedings of the Polymer Processing Society 26th Annual Meeting, Banff, AB, Canada, 4–8 July 2010.
26. Limper, A. *Mixing of Rubber Compounds*; Hanser Publishers: Munich, Germany, 2012; pp. 1–45. [[CrossRef](#)]
27. Limper, A.; Fischer, K. Processing of Natural Fibres in An Internal Mixer Opens up New Perspectives for Thermoplastic Lightweight Materials in the Automotive Industry. *Int. Polym. Sci. Technol.* **2015**, *42*, 1–4. [[CrossRef](#)]
28. Goris, S.; Back, T.; Yanev, A.; Brands, D.; Drummer, D.; Osswald, T.A. A novel fiber length measurement technique for discontinuous fiber-reinforced composites: A comparative study with existing methods. *Polym. Compos.* **2018**, *39*, 4058–4070. [[CrossRef](#)]
29. *DIN EN ISO 1172:2023-12*; Textilglasverstärkte Kunststoffe-Prepregs, Formmassen und Laminate-Bestimmung des Textilglas-und Mineralfüllstoffgehalts Mittels Kalzinierungsverfahren (ISO 1172:2023); Deutsche Fassung EN ISO 1172:2023. DIN Media GmbH: Berlin, Germany, 2023.
30. *DIN EN ISO 527-4:2022-03*; Kunststoffe-Bestimmung der Zugeigenschaften-Teil 4: Prüfbedingungen für Isotrop und Anisotrop Faserverstärkte Kunststoffverbundwerkstoffe (ISO 527-4:2021); Deutsche Fassung EN ISO 527-4:2021. Beuth Verlag GmbH: Berlin, Germany, 2022.

31. *DIN EN ISO 179-1:2023-10*; Kunststoffe-Bestimmung der Charpy-Schlageigenschaften-Teil 1: Nicht Instrumentierte Schlagzähigkeitsprüfung (ISO 179-1:2023); Deutsche Fassung EN ISO 179-1:2023. DIN Media GmbH: Berlin, Germany, 2023.
32. *DIN EN ISO 13802:2016-07*; Kunststoffe-Verifizierung von Pendelschlagwerken -Charpy-, Izod- und Schlagzugversuch (ISO 13802:2015, Korrigierte Fassung 2016-04-01); Deutsche Fassung EN ISO 13802:2015. DIN Media GmbH: Berlin, Germany, 2016.

**Disclaimer/Publisher's Note:** The statements, opinions and data contained in all publications are solely those of the individual author(s) and contributor(s) and not of MDPI and/or the editor(s). MDPI and/or the editor(s) disclaim responsibility for any injury to people or property resulting from any ideas, methods, instructions or products referred to in the content.